Iron environment non-equivalence in both octahedral and tetrahedral sites in NiFe 2 O 4 nanoparticles: Study using Mössbauer spectroscopy with a high velocity resolution

M. I. Oshtrakh, M. V. Ushakov, B. Senthilkumar, R. Kalai Selvan, C. Sanjeeviraja, and V. A. Semionkin

Citation: AIP Conference Proceedings **1489**, 115 (2012); doi: 10.1063/1.4759479
View online: http://dx.doi.org/10.1063/1.4759479
View Table of Contents: http://scitation.aip.org/content/aip/proceeding/aipcp/1489?ver=pdfcov
Published by the AIP Publishing

Iron Environment Non-Equivalence in Both Octahedral and Tetrahedral Sites in $NiFe_2O_4$ Nanoparticles: Study Using Mössbauer Spectroscopy with a High Velocity Resolution

M. I. Oshtrakh[a,b], M. V. Ushakov[a,b], B. Senthilkumar[c], R. Kalai Selvan[c], C. Sanjeeviraja[d] and V. A. Semionkin[a,b]

[a] *Department of Physical Techniques and Devices for Quality Control, Institute of Physics and Technology, Ural Federal University, Ekaterinburg, 620002, Russian Federation*
[b] *Department of Experimental Physics, Institute of Physics and Technology, Ural Federal University, Ekaterinburg, 620002, Russian Federation*
[c] *Solid State Ionics and Energy Devices Laboratory, Department of Physics, Bharathiar University, Coimbatore – 641 046, Indi.*
[d] *School of Physics, Alagappa University, Karaikudi – 630 006, Tamil Nadu, India*

Abstract. Mössbauer spectrum of $NiFe_2O_4$ nanoparticles was measured at room temperature in 4096 channels. This spectrum was fitted using various models, consisting of different numbers of magnetic sextets from two to twelve. Non-equivalence of the ^{57}Fe microenvironments due to various probabilities of different Ni^{2+} numbers surrounding the octahedral and tetrahedral sites was evaluated and at least 5 different microenvironments were shown for both sites. The fit of the Mössbauer spectrum of $NiFe_2O_4$ nanoparticles using ten sextets showed some similarities in the histograms of relative areas of sextets and calculated probabilities of different Ni^{2+} numbers in local microenvironments.

Keywords: Mössbauer spectroscopy, nickel ferrite nanoparticles, hyperfine parameters, ^{57}Fe in octahedral and tetrahedral sites.
PACS: 75.50.Gg, 76.80.+y

INTRODUCTION

Nickel ferrite ($NiFe_2O_4$) has an inverse spinel structure, Ni^{2+} cation occupies octahedral (B) sites and Fe^{3+} cation occupies both octahedral B and tetrahedral (A) sites. It was shown recently that $NiFe_2O_4$ nanoparticles appeared to be suitable electrodes for Li-ion batteries and supercapacitors [1–3] as well as for information storage, microwave devices, spintronics, and magnetic resonance imaging [4–6]. It is well-known that cation distribution affects the physical, chemical, and electrochemical properties of this material. Moreover, it is interesting to analyze Fe^{3+} local environment in both A and B sites. For this reason, application of Mössbauer spectroscopy is very useful. Various studies of nanosized $NiFe_2O_4$ particles using Mössbauer spectroscopy demonstrated the presence of two magnetic sextets with hyperfine magnetic fields in the ranges of about 500–550 kOe and 480–510 kOe for ^{57}Fe in the B and A sites, respectively (see, for instance, [7–10]). ^{57}Fe in the B sites

Mossbauer Spectroscopy in Materials Science - 2012
AIP Conf. Proc. 1489, 115-122 (2012); doi: 10.1063/1.4759479

demonstrated also larger isomer shift than that in the A sites. The authors of [7] demonstrated the fit of the Mössbauer spectrum of nanosized $NiFe_2O_4$ particles with accounting for two components related to the B and A sites in both surface shell and inner core of nanoparticles within the core-shell model. However, there were no attempts to analyze possible ^{57}Fe non-equivalence in the B and A sites due to variations in probabilities of different numbers of Ni^{+2} occupation of the B sites. Recently, we started application of Mössbauer spectroscopy with a high velocity resolution which appeared to be useful for the high quality spectra measurement [11,12]. For instance, using this technique, we fitted the Mössbauer spectrum of $CuFe_2O_4$ nanoparticles presented in 1024 channels using one magnetic sextet related to ^{57}Fe in the B site and two magnetic sextets related to ^{57}Fe in the A sites [13]. Therefore, we used Mössbauer spectroscopy with a high velocity resolution in the study of nanosized $NiFe_2O_4$ particles for analysis of ^{57}Fe in the B and A sites.

EXPERIMENTAL DETAILS

Nanosized $NiFe_2O_4$ particles were synthesized by solution combustion synthesis technique using 2.45 g of $Ni(NO)_2{\cdot}6H_2O$, 6.89 g of $Fe(NO)_3{\cdot}9H_2O$ and 2.49 g of EDTA ($C_{10}H_{16}N_2O_8$). EDTA was used as fuel and oxidant/fuel ratio was maintained at 1. The precursors were dissolved in double distilled water and pH was adjusted to 7 by an addition of ammonia solution. The solution was heated on hot plate. Initially, the temperature was maintained below 100 ºC to dehydrate the solution. After that, the temperature was suddenly increased to 300 ºC and auto-ignition took place with evolution of gases. The collected samples were calcined at 800 ºC for 5 hours.

The X-ray diffraction (XRD) patterns were collected using a powder X-ray diffractometer (PANalytical X'pert PRO) with CuK_α radiation and used to identify the phase composition. Investigation of the morphology of the prepared sample and their chemical composition was performed using a scanning electron microscopy (SEM) (Hitachi, Model S-3400N and Quanta 200 with an energy dispersion spectroscopy (EDS)) and transmission electron microscopy (TEM) (JEM 2011 type).

Mössbauer spectrum of the sample of $NiFe_2O_4$ nanoparticles (less than 14 mg Fe/cm^2) was measured using an automated precision Mössbauer spectrometric system built on the base of the SM–2201 spectrometer with a high velocity resolution. Details and characteristics of this equipment and the system were given elsewhere [12,14,15]. The Mössbauer spectrum was measured in transmission geometry with moving absorber in the cryostat at 295 K and recorded in 4096 channels. Spectrum was measured in velocity range of about ± 12 mm/s with a statistical rate of ~8.5×10^5 counts per channel in the spectrum and a signal-to-noise ratio of 48. The spectrum was computer fitted with the least squares procedure using the UNIVEM-MS program with a Lorentzian line shape. The ratio of sextet peaks areas was fixed as $S_{1,6}$:$S_{2,5}$:$S_{3,4}$=3:2:1 during the fit. The spectral parameters such as isomer shift, δ, quadrupole shift, ε, magnetic hyperfine field, H_{hf}, linewidth, Γ, relative subspectrum area, S, and statistical criterion, χ^2, were determined. An instrumental (systematic) error for each spectrum point was ± 0.5 channel (the velocity scale), the instrumental (systematic) error for the hyperfine parameters was ± 1 channel while the instrumental (systematic) error for a Γ evaluation was ± 2 channels. It should be noticed that spectrometer characteristics

determined an integral velocity error (total mechanical and electronics systematic and random errors) which was several times smaller than a half of channel value in mm/s during spectra measurements using 4096 channels [12,14]. If an error calculated with the fitting procedure (fitting error), for these parameters exceeded the instrumental (systematic) error we used the larger error instead. The velocity resolution (velocity per one channel) was ~0.006 mm/s per channel. The relative error for S did not exceed 10%. Differential spectra, χ^2 values, and physical meaning of the spectral parameters were used as criteria for the best fit. Value of a standard deviation (σ) of χ^2 was 0.022 for 4096 channels spectrum. Values of δ are given relative to α-Fe at 295 K.

RESULTS AND DISCUSSION

High intensity, sharp, and well-defined XRD peaks without any impurity peaks were observed for the prepared nanoparticles (see Fig. 1a) which indicated the high purity and the highly crystalline nature of $NiFe_2O_4$ spinel. The diffraction patterns provide clear evidence for the formation of cubic spinel structure and are in very good agreement with the reported values (JCPDS card No.44-1485). SEM image of $NiFe_2O_4$ nanoparticles is shown in Fig. 1b. Chemical analysis of this sample showed the following average composition: O – 42 at.%, Fe – 39 at.%, and Ni – 19 at.%. TEM image of $NiFe_2O_4$ nanoparticles is shown in Fig. 1c. The average particles size was evaluated to be about 15 nm.

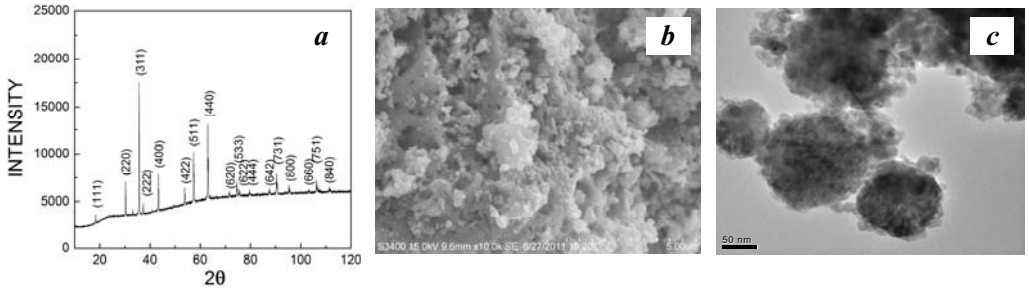

FIGURE 1. (a) X-ray diffraction patterns, (b) SEM, (c) and TEM images of $NiFe_2O_4$ nanoparticles.

Mössbauer spectrum of $NiFe_2O_4$ nanoparticles registered in 4096 channels is shown in Fig. 2. This spectrum looks like spectra of similar compounds and visually consists of two sextets. Evaluated Mössbauer parameters for the component 1 were $\Gamma = 0.396 \pm 0.012$ mm/s, $\delta = 0.339 \pm 0.006$ mm/s, $\varepsilon = -0.066 \pm 0.006$ mm/s, $H_{hf} = 513.1 \pm 0.2$ kOe, $S = 46\%$ and those for the component 2 were $\Gamma = 0.484 \pm 0.012$ mm/s, $\delta = 0.233 \pm 0.006$ mm/s, $\varepsilon = -0.035 \pm 0.006$ mm/s, $H_{hf} = 480.7 \pm 0.2$ kOe, $S = 54\%$ ($\chi^2 = 1.674$). These values were similar to previously reported (see, for instance, [8–10]). However, the fit of the measured spectrum using two magnetic sextets was not satisfactory as clearly seen in Fig. 2 using the differential spectrum. Further, spectrum fits were carried out using various numbers of magnetic sextets up to twelve. Differential spectra demonstrated better quality of fit with a decrease in χ^2 values (for instance, 1.307 for six sextets, 1.270 for seven sextets, 1.230 for eight sextets, 1.190 for ten sextets and 1.168 for twelve sextets). A decrease in χ^2 values with the next sextet

addition for the fitting model was larger than σ while differential spectra appeared to be similar in the fits using ten–twelve sextets.

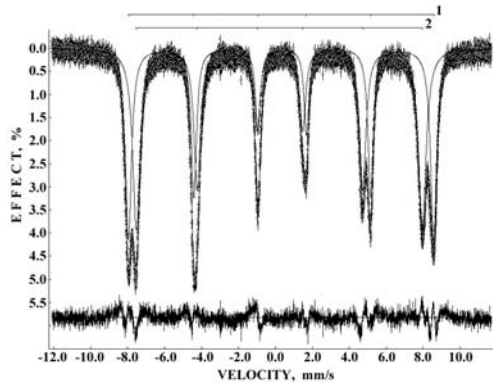

FIGURE 2. Mössbauer spectrum of $NiFe_2O_4$ nanoparticles measured in 4096 channels at 295 K and fitted using two magnetic sextets related to ^{57}Fe in the octahedral and tetrahedral sites. Differential spectrum is shown below.

To analyze the necessity of more than two sextets required for the better fit of Mössbauer spectrum of $NiFe_2O_4$ nanoparticles, we evaluated probabilities of various Ni^{2+} numbers in the local environment of the A and B sites. For this reason, we calculated these probabilities for ^{57}Fe in both A and B sites of the $NiFe_2O_4$ unit cell within the spheres with different radii, i.e., 3.7 Å, 3.5 Å, and 3.3 Å. The local environments of Fe^{3+} in both A and B sites within the sphere with a radius of 3.7 Å are shown in Fig. 3.

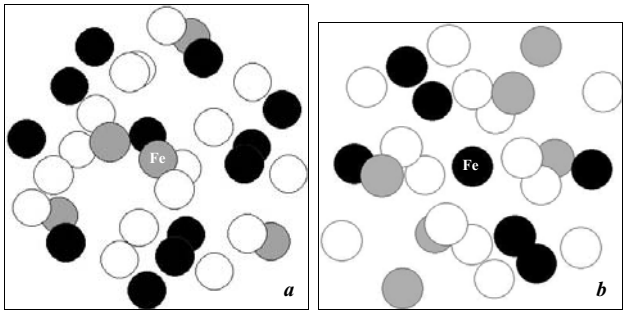

FIGURE 3. Local environments of Fe^{3+} in both (a) A and (b) B sites within the sphere with a radius of 3.7 Å: ○ – oxygen atoms, ● – Fe^{3+} in the A sites, ● – Fe^{3+} or Ni^{2+} in the B sites.

Calculated numbers of atoms and sites in the local environment within spheres with different radii for each site are given in Table 1. Calculated probabilities of different numbers of Ni^{2+} in the local environment of ^{57}Fe in both A and B sites are shown in Fig. 4. On the basis of calculated probabilities (if ≥ 0.05), we can suppose that within a sphere of 3.7 Å radius, it may be possible to consider seven non-equivalent micro-environments for ^{57}Fe in the tetrahedral sites and five non-equivalent micro-environments for ^{57}Fe in the octahedral sites while within the sphere of 3.5 Å radius, it

may be possible to consider five different microenvironments for the ^{57}Fe in the tetrahedral sites and five different microenvironments for ^{57}Fe in the octahedral sites.

TABLE 1. Local environment for tetrahedral and octahedral sites in $NiFe_2O_4$.

Sphere radius (Å)	Number of O atoms	Number of A sites (Fe^{3+})	Number of B sites (Fe^{3+} and Ni^{2+})
Tetrahedral site (A)			
3.3	6	0	0
3.5	16	0	8
3.7	16	4	12
Octahedral site (B)			
3.3	6	0	6
3.5	8	6	6
3.7	14	6	6

In the case of local microenvironment within a sphere of 3.3 Å radius, calculated probabilities predicted one microenvironment for ^{57}Fe in the A site and five different microenvironments for ^{57}Fe in the B site. Thus, for comparison, we chose three fits of the Mössbauer spectrum of $NiFe_2O_4$ nanoparticles using twelve, ten, and six sextets.

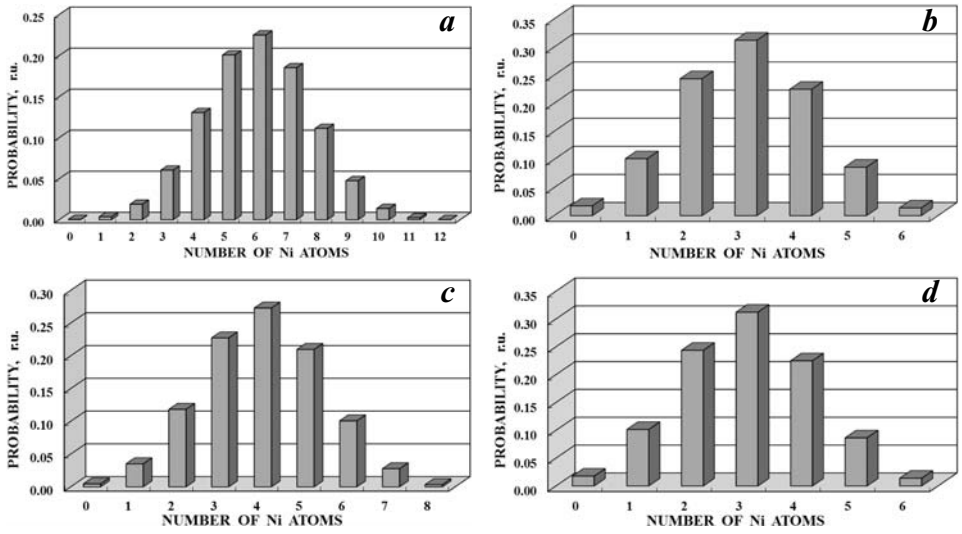

FIGURE 4. Histograms of the probabilities of various numbers of Ni^{2+} in the local environment of ^{57}Fe in the $NiFe_2O_4$ unit cell in both (a) A and (b) B sites within the sphere with a radius of 3.7 Å and in both (c) A and (d) B sites within the sphere with a radius of 3.5 Å.

The obtained parameters of the fits using twelve and ten sextets are collected in Table 2 and shown in Fig. 5. Non-equivalent ^{57}Fe microenvironments were denoted as sites B1, B2, etc., and A1, A2, etc. Each sextet was related to ^{57}Fe in the octahedral or tetrahedral sites on the basis of the values of H_{hf} and δ; the largest values of these parameters were related to ^{57}Fe in the octahedral sites while the lower values were related to ^{57}Fe in the tetrahedral sites. In the case of six sextets fit, Mössbauer parameters of three sextets demonstrated parameters corresponding to ^{57}Fe in the tetrahedral sites in contrast to calculated one microenvironment for the tetrahedral site. Therefore, this fit was omitted from further consideration.

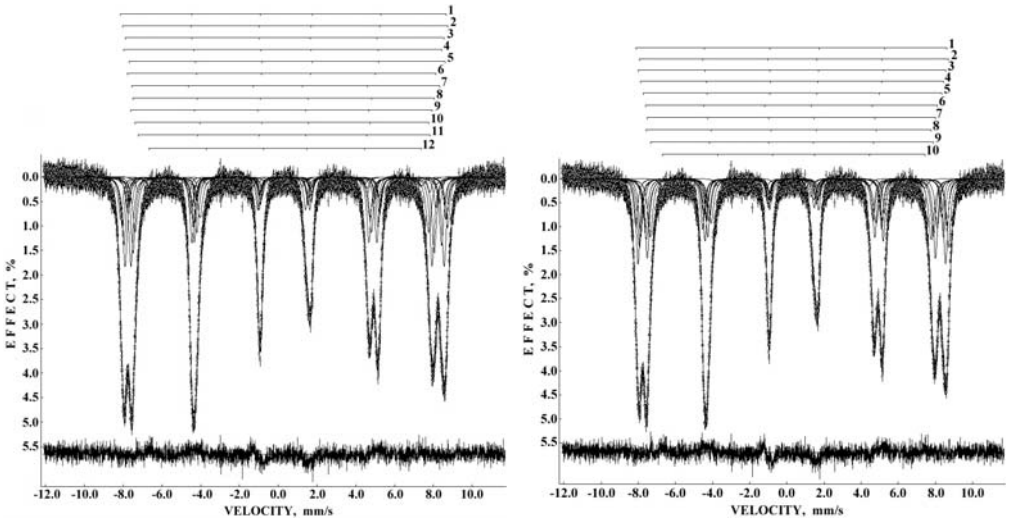

FIGURE 5. Mössbauer spectrum of $NiFe_2O_4$ nanoparticles measured in 4096 channels at 295 K and fitted using twelve magnetic sextets (left) and ten magnetic sextets (right) related to ^{57}Fe in the octahedral and tetrahedral sites. Differential spectra are shown below.

TABLE 2. Values of the Mössbauer parameters for $NiFe_2O_4$ nanoparticles derived from spectrum fits using twelve and ten sextets.

No[a]	Γ (mm/s)	δ (mm/s)	E (mm/s)	H_{hf} (kOe)	S (%)	χ^2	^{57}Fe in site
1	0.253 ± 0.019	0.334 ± 0.006	– 0.157 ± 0.016	521.3 ± 0.4	6.78	1.168	B1
2	0.257 ± 0.019	0.355 ± 0.006	– 0.017 ± 0.014	520.8 ± 0.3	8.27		B2
3	0.274 ± 0.016	0.322 ± 0.006	0.010 ± 0.007	511.0 ± 0.2	15.50		B3
4	0.257 ± 0.020	0.315 ± 0.006	– 0.174 ± 0.012	509.0 ± 0.3	11.15		B4
5	0.257 ± 0.020	0.455 ± 0.010	– 0.001 ± 0.022	506.2 ± 0.9	4.36		B5
6	0.252 ± 0.012	0.305 ± 0.006	– 0.028 ± 0.006	494.4 ± 0.4	5.18		A1
7	0.247 ± 0.035	0.184 ± 0.006	0.414 ± 0.017	493.4 ± 0.7	4.09		A2
8	0.274 ± 0.014	0.293 ± 0.006	– 0.026 ± 0.006	482.5 ± 0.3	13.19		A3
9	0.265 ± 0.014	0.171 ± 0.006	– 0.008 ± 0.006	482.3 ± 0.3	15.05		A4
10	0.337 ± 0.018	0.267 ± 0.006	– 0.161 ± 0.011	470.1 ± 0.5	11.77		A5
11	0.254 ± 0.044	0.251 ± 0.011	– 0.083 ± 0.029	467.3 ± 1.1	2.44		A6
12	0.363 ± 0.045	0.361 ± 0.012	– 0.011 ± 0.023	436.4 ± 1.0	2.22		A7
1	0.252 ± 0.012	0.337 ± 0.006	– 0.182 ± 0.008	520.3 ± 0.3	7.69	1.190	B1
2	0.272 ± 0.012	0.341 ± 0.006	0.103 ± 0.006	516.6 ± 0.2	12.03		B2
3	0.252 ± 0.012	0.336 ± 0.006	– 0.123 ± 0.006	514.4 ± 0.4	13.84		B3
4	0.252 ± 0.012	0.342 ± 0.006	– 0.118 ± 0.007	506.3 ± 0.5	9.51		B4
5	0.253 ± 0.025	0.340 ± 0.006	– 0.035 ± 0.009	498.8 ± 0.5	6.29		B5
6	0.294 ± 0.018	0.163 ± 0.007	0.190 ± 0.011	487.8 ± 0.4	9.25		A1
7	0.272 ± 0.013	0.248 ± 0.006	– 0.001 ± 0.006	481.9 ± 0.3	13.94		A2
8	0.351 ± 0.014	0.243 ± 0.006	– 0.262 ± 0.017	476.5 ± 0.6	13.63		A3
9	0.314 ± 0.014	0.258 ± 0.006	0.039 ± 0.007	473.4 ± 0.4	11.65		A4
10	0.355 ± 0.043	0.371 ± 0.012	– 0.006 ± 0.023	438.7 ± 1.0	2.17		A5

[a] Numbers of components in Fig. 4 (left and right, respectively).

In these fits, the total areas of magnetic components related to the octahedral and tetrahedral sites in these fits were found to be ~46.1% and ~53.9% (twelve sextets fit), respectively, and ~49.4% and ~50.6% (ten sextets fit), respectively. These results are in agreement with stoichiometry of $NiFe_2O_4$ nanoparticles determined by the local

chemical analysis. It is interesting to compare corresponding histograms of the probabilities of the numbers of Ni^{2+} in the ^{57}Fe local microenvironments and histograms of relative areas of sextets versus magnetic hyperfine fields. If we suppose that an increase in the Ni^{2+} number in the local microenvironment of ^{57}Fe leads to a decrease in the magnetic hyperfine field, the components with the largest values of H_{hf} may be related to the local microenvironment without Ni^{2+} while the lowest ones may be related to the maximum number of Ni^{2+} in both octahedral and tetrahedral sites within the chosen sphere (see obtained histograms of relative areas in Fig. 6). Comparison of corresponding histograms in Fig. 4 and Fig. 6 demonstrated some similarities which may confirm the presence of more than two sextets in the Mössbauer spectrum of $NiFe_2O_4$ nanoparticles. Further, one can analyze the Mössbauer parameters given in Table 2 to choose the most appropriate fit. It is clearly seen that several values of H_{hf} for some pairs of spectral components obtained using twelve sextets fit were the same within the error. This rise some doubts in physical meaning of these parameters. In contrast, there are not the same values of H_{hf} for any pair of components obtained using ten sextets fit. Therefore, we can suppose that this fit may be considered as the most appropriate one.

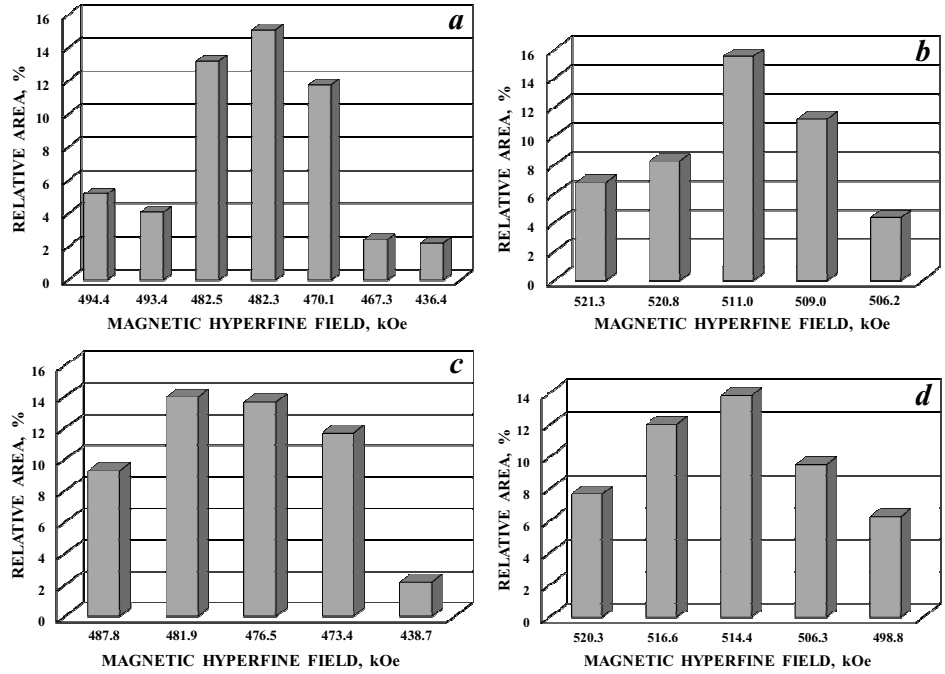

FIGURE 6. Histograms of relative areas of magnetic components in the Mössbauer spectrum of $NiFe_2O_4$ nanoparticles obtained from the fit using twelve sextets and related to ^{57}Fe in both (a) A and (b) B sites and from the fit using ten sextets and related to ^{57}Fe in both (c) A and (d) B sites.

CONCLUSIONS

Study of $NiFe_2O_4$ nanoparticles using Mössbauer spectroscopy with a high velocity resolution demonstrated the necessity of more than two magnetic sextets for the better

spectrum fit. An analysis of probabilities of different numbers of Ni^{2+} in the local microenvironment of ^{57}Fe in both octahedral and tetrahedral sites demonstrated non-equivalence of ^{57}Fe microenvironments. The histograms of these probabilities were similar to the histograms of relative areas of magnetic components obtained from the better fits. Taking into account physical meaning of Mössbauer parameters, we choose the fit using ten magnetic sextets that may correspond to the different local microenvironments of ^{57}Fe in both octahedral and tetrahedral sites within the sphere with a radius of 3.5 Å. These results demonstrated the necessity of accounting for the iron microenvironment non-equivalence in both octahedral and tetrahedral sites in the fit of Mössbauer spectra of $NiFe_2O_4$ nanoparticles; however, further investigations are required.

ACKNOWLEDGMENTS

This work was supported in part by the Ministry of Science and Education of Russian Federation.

REFERENCES

1. H. Zhao, Z. Zheng, K. Wai and S. Wang, *Electrochem. Commun.* **9**, 2606–2610 (2007).
2. P. Sen and A. De, *Electrochimi. Acta* **55**, 4677– 4684 (2010).
3. A. Anwar, K. S. Muthu, V. Ganesh and Lakshminarasimhan, *J. Electrochem. Soc.* **158**, A976–A981 (2011).
4. U. Luders, A. Barthelemy, M. Bibes, K. Bouzehouane, S. Fusil, E. Jacquet, J.-P. Contour, J.-F. Bobo, J. Fntcuberta and A. Fert, *Adv. Mater*. **18**, 1733–1736 (2006).
5. V. Šepelák, D. Baabe, D. Mienert, D. Schultze, F. Krumeich, F. J. Litterst and K. D. Becker, *J. Magn. Mag. Mater.* **257**, 377–386 (2003).
6. E. F. Schloemann, *Mag. Mater.* **209**, 15–20 (2000).
7. V. Šepelák, I. Bergmann, A. Feldhoff, P. Heitjans, F. Krumeich, D. Menzel, F. J. Litterst, S. J. Campbell and K. D. Becker, *J. Phys. Chem. C* **111**, 5026–5033 (2007).
8. M. A. F. Ramalho, L. Gama, S. G. Antonio, C. O. Paiva-Santos, E. J. Miola, R. H. G. A. Kiminami and A. C. F. M. Costa, *J. Mater. Sci*. **42**, 3603–3606 (2007).
9. S. S. Umare, R. S. Ningthoujam, S. J. Sharma, S. Shrivastava, S. Kurian and N. S. Gajbhiye, *Hyperfine Interact*. **184**, 649–657 (2008).
10. B. Y. Yu and S.-Y. Kwak, *Dalton Trans.* **40**, 9989–9998 (2011).
11. M. I. Oshtrakh, V. A. Semionkin, V. I. Grokhovsky, O. B. Milder and E. G. Novikov, *J. Radioanal. Nucl. Chem*. **279**, 833–846 (2009).
12. M. I. Oshtrakh and V. A. Semionkin, *Spectrochim. Acta Pt. A-Molec. Biomolec. Spectr.,* doi: 10.1016/j.saa.2012.03.020 (2012).
13. M. I. Oshtrakh, R. K. Selvan, C. O. Augustin and V. A. Semionkin, *Hyperfine Interact*. **183**, 37–34 (2008).
14. M. I. Oshtrakh, V. A. Semionkin, O. B. Milder and E. G. Novikov, *J. Radioanal. Nucl. Chem*. **281**, 63–67 (2009).
15. V. A. Semionkin, M. I. Oshtrakh, O. B. Milder and E. G. Novikov, *Bulletin of the Russian Academy of Sciences. Physics* **74**, 416–420 (2010).